

Periodic boundary conditions and G_2 cosmology

A A Coley,

Department of Mathematics & Statistics, Dalhousie University,
Halifax, Nova Scotia, Canada B3H 3J5
Email: acoley@dal.ca

W C Lim,

Department of Mathematics, University of Waikato, Private Bag 3105, Hamilton 3240, New Zealand
Email: wclim@waikato.ac.nz

Abstract

In the standard concordance cosmology the spatial curvature is assumed to be constant and zero (or at least very small). In particular, in numerical computations of the structure of the universe using N-body simulations, exact periodic boundary conditions are assumed which constrains the spatial curvature. In order to confirm this qualitatively, we numerically evolve a special class of spatially inhomogeneous G_2 models with both periodic initial data and non periodic initial data using zooming techniques. We consequently demonstrate that in these models periodic initial conditions do indeed suppress the growth of the spatial curvature as the models evolve away from their initial isotropic and spatially homogeneous state, thereby verifying that the spatial curvature is necessarily very small in standard cosmology.

1 Introduction

Cosmology is concerned with the large scale behaviour of the Universe within General Relativity (GR) [1]. The *cosmological principle* then implies that on the largest scales the Universe can be accurately modeled by an exact solution to Einstein's field equations (EFE) which is both spatially homogeneous and isotropic leading to a (background) Friedmann-Lemaître-Robertson-Walker (FLRW) model (with constant spatial curvature) with the cosmological constant, Λ , representing dark energy (or the so-called Λ CDM standard concordance cosmology, where CDM denotes cold dark matter). Inflation in the early universe is often regarded as a part of the standard model, in which the background spatial curvature, characterized by the normalized curvature parameter, is predicted to be negligible [2]. Regardless of whether inflation is included as part of the standard model or not, spatial curvature is implicitly assumed to be zero.

An important goal in cosmology is to understand the origin of the structure of the universe. Assuming that cosmic structure grew out of small initial fluctuations, we can investigate their evolution on sufficiently large scales using linear perturbation theory (LPT), where the spatially inhomogeneous perturbations *live* on the flat FLRW background spacetime. Inflation then provides a causal mechanism for generating primordial cosmological perturbations via quantum fluctuations in the inflaton field, which subsequently act as seeds for the anisotropies in the cosmic microwave background (CMB) [3] and give rise to the large scale structure of our universe. At late times and scales much smaller than the Hubble scale fluctuations of the cosmic density are not necessarily small, and LPT is not sufficient and clustering needs to be treated non-linearly. Usually this is studied with (non-relativistic) N-body simulations. Recently non-linear perturbations have been investigated at second-order and non perturbative relativistic effects have been studied computationally [1].

Although standard cosmology has been very successful in describing current observations, there are a number of possible anomalies [4], including the tension between the recent determination of the local value of the Hubble constant based on direct measurements of supernovae [5] and the value derived from the most recent CMB data [3], as well as various self-inconsistencies [6]. In addition, the values of cosmological parameters inferred from the CMB perhaps suggest a number of directional dependences (e.g., possible greater than anticipated bulk flows on large scales and *dark flow* [7]).

In principle, since the Universe is not isotropic or spatially homogeneous on small local scales, the effective smoothed out macroscopic gravitational FE on large scales should be obtained by averaging the EFE of GR. The averaging of the EFE for local inhomogeneities can lead to important backreaction

effects on the average evolution of the Universe [8], and can significantly affect precision cosmology at the level of 1 % [1].

1.1 Spatial curvature

As noted above, in standard cosmology the spatial curvature is assumed to be constant and zero (or at least perturbatively small).¹ However, there is no completely independent constraint that guarantees a value for the magnitude of the effective normalized spatial curvature Ω_k of less than about 1 %. Moreover, any possible such small non-zero measurement of Ω_k can perhaps be taken to indicate that the assumptions in the standard model are not valid. We also note that spatial curvature is, in general, evolving in relativistic cosmological models [8].

In order to develop models to be utilized for cosmological predictions and comparison with observational data, it is necessary to make assumptions. However, it is crucial to check how the assumptions affect the results. More importantly, we can only validate the consistency of assumptions and we cannot rule out alternative explanations. The assumption of a FLRW background on cosmological scales presents a number of problems [1]. For example, the assumption that there exists a 1+3 spacetime split and a global time and a background inertial (Gaussian normal) coordinate system over a complete Hubble scale *background* patch in the standard model leads to the constraint that the spatial curvature (and the vorticity) must be sufficiently small. In addition, any assumptions of exact periodic boundary conditions (PBC) (appropriate on scales comparable to the homogeneity scale) necessarily imply that the global spatial curvature is exactly zero [1] (since in the actual standard model the Universe is taken to be simply connected), and thus any suitable approximation will amount to Ω_k being less than the perturbation (e.g., LPT) scale. We shall return to this point below.

There are also assumptions related to the weak field approach, the actual applicability of perturbation theory and Gaussian initial conditions, that imply spatial curvature is neglected. It is also asserted that cosmological backreaction can be neglected, but in LPT the initial fluctuations are usually taken to be Gaussian, which implies that at the linear level all averages are zero by construction. In addition, we should be aware that any intuition based on Newtonian theory may be misplaced; e.g., the average spatial curvature of voids and clustered matter (with negative and positive curvature, respectively) is not necessarily zero within GR. Thus, within standard cosmology the spatial curvature is assumed to be zero, or at least very small and at most first order in terms of the perturbation approximation, in order for any subsequent analysis to be valid. Any prediction larger than this indicates an inconsistency in the approach. In this sense the standard model cannot be used to predict a small spatial curvature.

It has recently been re-emphasized that, in an era of precision cosmology, any physical approximations (including, for example, the use of LPT), in standard cosmological models should be analysed to check if they are sufficiently accurate for comparison with observations used to draw conclusions about the actual properties of our Universe [9].

1.2 Periodic boundary conditions

In the general inhomogeneous cosmological case, the formulation of the evolution eqns. consists of utilizing global Cartesian coordinates and metric variables, where initial conditions on the metric are specified. In the actual N-body simulations a cell of length L (a fraction of the Hubble scale) is taken and the system is integrated where the PBC at L is applied at all times (and is used at every step to compute spatial derivatives near the edges of the cell). Hence spatial curvature is held zero on the boundary, and in this sense the growth of spatial curvature is suppressed, relatively speaking. It is of importance to verify numerically that initial PBC constrain the spatial curvature to be zero at the boundary for all time, which is maintained at zero even below numerical errors that begin to grow.

In addition, if in N-body simulations the cell is restricted to a finite size L, then periodicity implies that longer wavelength inhomogeneities than L are effectively neglected. This will have an effect on the numerical simulations, which is a general concern, especially when the large-scale cutoff is indeed below

¹By *global* constant spatial curvature we essentially mean the value of k in the background FLRW spacetime (and hence the initial conditions). By the *local* value of the spatial curvature we primarily mean the local value obtained later in the paper by the numerical integration across the region of simulation for different specific values of x_{zoom} . In the later numerical simulations we also discuss an averaged spatial curvature at a given time.

the Hubble scale as will be necessary if small ($\sim Mpc$) scales are to be resolved. (There will be a cutoff in practice in the power spectrum of the inhomogeneities immediately from the initial conditions.)

Finally, it is not absolutely clear whether periodic initial conditions guarantee periodic evolution for all times. There is no general mathematical theorem on the preservation of discrete symmetries (that periodicity implies; however, see [10]). But note that if it were true that periodic initial conditions are propagated, then it follows that the spatial curvature is indeed constrained at L for all times.

In the few current relativistic cosmological simulations, the spatial curvature can have large local fluctuations but remains small when averaged over large scales. It becomes extremely small, $\Omega_R \sim 10^{-8}$, when averaged over the whole periodic box of the simulation [11]. Work is in progress for a more in-depth investigation of average spatial curvature from numerical relativity, along with the constraints due to the PBC, in a more frame-independent formalism [12]. However, the preliminary evidence is that these numerical solutions have an exceptionally and unnaturally small spatial curvature in a neighbourhood of the periodic boundary, which affects the average spatial curvature in the whole cell, and can perhaps be ascribed to the use of PBC.

In different formulations of the EFE (e.g., the G_2 case below), it is difficult to compare with the standard numerical results of the full 3D code and the usual N-body simulations. Indeed, since the EFE are hyperbolic, and depending on the particular formulation of the evolution equations, once the initial conditions are fully specified it is not clear whether the application of spatial PBC are even required (beyond the specification of the initial data that is).

2 Spatially inhomogeneous models

The FLRW cosmology (or Friedmann–Lemaître (FL) model as we will refer to as here when regarding the solution as a dynamical equilibrium state) is an expanding exactly spatially homogeneous and spatially isotropic universe, which is believed to describe the Universe on a sufficiently large spatial scale, at least since the time of last scattering. However, the observable part of the Universe is not exactly spatially homogeneous and isotropic on any spatial scale. From a practical point of view, we are interested in studying models that are *close to FL* in some appropriate dynamical sense, perhaps using deviations from an FL model by applying LPT. But it is not known how reliable the linear theory is and, moreover, in using it we are a priori excluding the possibility of uncovering important non-linear effects.

Therefore, it is of interest to consider (more) general spatially inhomogeneous models (than FL) in order to investigate the constraints that observations impose [13]. Indeed, it could be argued that we should not study exotic ideas until conventional GR (with inhomogeneities) has been fully explored. In the first instance, it is perhaps advisable to investigate a special inhomogeneous model where some analytical and qualitative insights are possible. In this paper we wish to *study the effect of spatial curvature and PBC numerically in the special case of G_2 models*.

2.1 G_2 models

The simplest spatially inhomogeneous cosmological models have two commuting Killing vector fields (i.e., models admitting a 2-parameter Abelian isometry group acting transitively on spacelike 2-surfaces), which consequently have a single degree of spatial inhomogeneity. This class of models, which are referred to briefly as G_2 cosmologies, are governed by the EFE which constitute partial differential equations (PDE) in two independent variables [14]. A lot of the research to date has focused on the so-called Gowdy vacuum spacetimes [15], because such models are much more tractable than non-vacuum ones and the existence of compact space sections facilitates numerical simulations since the problem of boundary conditions at spatial infinity is avoided. Recently, a plane-parallel model (or wall universe) [16], in which light rays pass through a series of plane-symmetric perturbations around a FLRW background, was used to study the back-reaction from the small-scale inhomogeneities [17, 18].

Belinskii, Khalatnikov and Lifshitz (BKL) [19] have conjectured that within GR the approach to the generic spacelike singularity to the past is vacuum dominated (assuming $p < \rho$), local, and oscillatory (labeled ‘Mixmaster’). Localilty implies that the contribution of terms in the evolution eqns. with spatial derivatives can be neglected. Numerical studies of the asymptotics of the simplest inhomogeneous vacuum Gowdy models demonstrate that on approach to the singularity, spiky structures form [20]. These spikes become narrower as the singularity is approached. Studies of G_2 and more general models have produced

numerical evidence that the BKL conjecture generally holds except possibly at isolated points where spiky structures form [21, 22].

We are particularly interested in late time evolution here. We shall concentrate on G_2 cosmologies with a perfect fluid matter content, and especially dust [23]. At any instant of time, the state of a G_2 cosmology is described by a finite-dimensional dynamical state vector of functions of the spatial coordinate. That is, the dynamical state space of G_2 cosmologies is a function space and is thus infinite-dimensional. The evolution of a G_2 cosmology is consequently described by an orbit in this infinite-dimensional dynamical state space. In a G_2 cosmology, at each point there exists a preferred timelike 2-space that is orthogonal to the G_2 -orbits. Therefore, there is an infinite family of geometrically preferred timelike congruences and gauge freedom in the choice of the orthonormal frame (and associated with the choice of the local coordinates). Following [24, 14], we shall utilize the orthonormal frame formalism adapted to the G_2 orbits. Such a dynamical formulation has proved effective in studying G_2 cosmologies. Here we define scale-invariant dependent variables by normalisation with the area expansion rate of the G_2 -orbits, in order to obtain the evolution eqns. as a system of PDE in first-order symmetric hyperbolic (FOSH) format. This FOSH format also provides a natural framework for numerical studies.

2.2 G_2 evolution equations in timelike area gauge

The geometry of the general G_2 class of spacetimes is given in [22], where all of the metric functions depend only on the time coordinate t and the spatial coordinate x . We will display the G_2 evolution system in terms of the timelike area gauge in the Gowdy subcase $\Sigma_2 = 0$ (with unit lapse, thereby defining t time). We utilize β -normalized variables [14, 23] in the orthonormal frame formalism [24], where the t and x subscripts denote partial differentiation. We also assume dust ($\gamma = 1$) and a single non-zero tilt component, v . We are particularly interested in future dynamics close to 'FL'. We also assume that the cosmological constant is zero, so that we have an unconstrained evolution system in FOSH format [14]:

$$\partial_t E_1^1 = (q + 3\Sigma_+) E_1^1 \quad (1)$$

$$\partial_t \Sigma_- + E_1^1 \partial_x N_\times = (q + 3\Sigma_+ - 2) \Sigma_- + 2\sqrt{3} \Sigma_\times^2 - 2\sqrt{3} N_-^2 \quad (2)$$

$$\partial_t N_\times + E_1^1 \partial_x \Sigma_- = (q + 3\Sigma_+) N_\times \quad (3)$$

$$\partial_t \Sigma_\times - E_1^1 \partial_x N_- = (q + 3\Sigma_+ - 2 - 2\sqrt{3}\Sigma_-) \Sigma_\times - 2\sqrt{3} N_\times N_- \quad (4)$$

$$\partial_t N_- - E_1^1 \partial_x \Sigma_\times = (q + 3\Sigma_+ + 2\sqrt{3}\Sigma_-) N_- + 2\sqrt{3} \Sigma_\times N_\times \quad (5)$$

$$(\partial_t + v E_1^1 \partial_x) \Omega + \Omega E_1^1 \partial_x v = 2 \Omega [(q + 1) - \frac{1}{2} (1 - 3\Sigma_+) (1 + v^2) - 1] \quad (6)$$

$$(\partial_t + v E_1^1 \partial_x) v = (1 - v^2) [3(N_\times \Sigma_- - N_- \Sigma_\times) + \frac{3}{2} \Omega v - (1 - 3\Sigma_+) v] \quad (7)$$

where

$$(q + 3\Sigma_+) \equiv 2 - \frac{3}{2} (1 - v^2) \Omega \quad (8)$$

and

$$\Sigma_+ \equiv \frac{1}{2} (1 - \Sigma_-^2 - N_\times^2 - \Sigma_\times^2 - N_-^2 - \Omega). \quad (9)$$

Note that in the present case we have from Eqs. (ca:q3sigp) and (ca:sigpt) that

$$q = \frac{1}{2} + \frac{3}{2} (\Sigma_-^2 + N_\times^2 + \Sigma_\times^2 + N_-^2) + \frac{3}{2} v^2 \Omega \geq \frac{1}{2}, \quad (10)$$

which, together with

$$\partial_t \beta = -(q + 1) \beta, \quad (11)$$

guarantees that β is single signed and is monotone (for small ϵ – see below). The (negative) spatial curvature ($-\Omega_k$) is defined via

$$\Omega_k \equiv N_\times^2 + N_-^2. \quad (12)$$

The relation of the variables above with metric components is given by (see (6.39) and (6.40) of [23], or Appendix A.3 of [14]):

$$ds^2 = \beta^{-2} [-dt^2 + (E_1^1)^{-2} dx^2] + e^{2t} [e^{P(t,x)} (dy + Q(t,x) dz)^2 + e^{-P(t,x)} dz^2] \quad (13)$$

$$(\Sigma_-, N_\times) = \frac{1}{2\sqrt{3}}(\partial_t, -E_1^1 \partial_x)P \quad (14)$$

$$(\Sigma_\times, N_-) = \frac{1}{2\sqrt{3}}e^P(\partial_t, E_1^1 \partial_x)Q. \quad (15)$$

2.2.1 Initial data

Since we have an unconstrained FOSH system no constraints need be satisfied and we freely specify $\{E_1^1, \Sigma_-, N_\times, \Sigma_\times, N_-, \Omega, v\}$ at $t = 0$ on $\{-L \leq x \leq L\}$.

We shall consider initial data close to a (flat) FL model of the form (for small $\epsilon \sim 10^{-4}$):

$$\begin{aligned} \{E_1^1 = 1 + \epsilon^2 \tilde{E}\}, \\ \{\Sigma_- = \epsilon \tilde{\Sigma}_-, N_\times = \epsilon \tilde{N}_\times, \Sigma_\times = \epsilon \tilde{\Sigma}_\times, N_- = \epsilon \tilde{N}_-\}, \\ \{\Omega = 1 - \epsilon^2 \tilde{\Omega}, v = \epsilon^2 \tilde{v}\}. \end{aligned}$$

Note that it follows that

$$\{q = \frac{1}{2} + \epsilon^2 \tilde{q}, \Sigma_+ = \epsilon^2 \tilde{\Sigma}_+, \Omega_k = \epsilon^2 \tilde{\Omega}_k\}.$$

The initial data is given by (for example) $\epsilon \tilde{\Sigma}_-$ at $t = 0$ (etc.). Since shell crossings can occur in dust models, we either cease integration once any singular behaviour develops or we can include a small fiducial pressure in the models.

2.2.2 Linear regime

For small ϵ , we integrate eqn. (1) to obtain:

$$\tilde{E} = e^{\frac{t}{2}} + o(\epsilon^2), \quad (16)$$

where we have normalized \tilde{E} to be unity at $t = 0$. In the linear regime we have that $e^{\frac{t}{2}}$ is small (which for $\epsilon \sim 10^{-4}$ corresponds to $t < 10$). Eqns. (6,7) also constitute $o(\epsilon^2)$ corrections to zeroth order evolution equations. In the linear regime, $\Omega_k \sim o(\epsilon^2)$.

2.2.3 Shear and curvature

Eqns. (2) – (5) represent the first order evolution eqns. for the normalized shear and curvature variables with second order corrections. We immediately see the growing modes for the normalized curvature variables $\sim e^{\frac{t}{2}}$ and the decaying modes for the normalized shear variables $\sim e^{-\frac{3t}{2}}$, corresponding to the familiar eigenvalues $\{\frac{1}{2}, -\frac{3}{2}\}$ for the flat FL "saddle point" solution [so that the growth of the shear is suppressed relative to that of the spatial curvature in the initial linear regime].

Solving eqns. (2) - (5) we obtain:

$$\tilde{\Sigma}_- = e^{-\frac{3t}{2}}[\sigma_- + \epsilon \bar{\Sigma}_-], \quad (17)$$

$$\tilde{N}_\times = e^{\frac{t}{2}}[\nu_\times + \epsilon \bar{N}_\times], \quad (18)$$

$$\tilde{\Sigma}_\times = e^{-\frac{3t}{2}}[\sigma_\times + \epsilon \bar{\Sigma}_\times], \quad (19)$$

$$\tilde{N}_- = e^{\frac{t}{2}}[\nu_- + \epsilon \bar{N}_-], \quad (20)$$

where $\{\sigma_-, \sigma_\times, \nu_-, \nu_\times\}$ are slowly varying (and, for example, $\partial_x \Sigma_- \sim (\epsilon e^{\frac{t}{2}}) \bar{\Sigma}_-'$, $\partial_x \Sigma_\times \sim (\epsilon e^{\frac{t}{2}}) \bar{\Sigma}_\times'$, where a prime denotes ∂_x). In the regime in which the shear is sub-dominant, these quantities are approximately constant.

2.2.4 Spatial curvature

From eqns. (3) and (5), to $o(\epsilon)$ eqn. (12) becomes:

$$\partial_t \Omega_k = \Omega_k, \quad (21)$$

so that Ω_k remains small (and of second order initially). More precisely, to $o(\epsilon^4)$:

$$\partial_t \Omega_k = (\epsilon e^{\frac{t}{2}})^2 [(\nu_-^2 + \nu_\times^2) + \epsilon(\nu_\times \bar{N}_\times + \nu_- \bar{N}_-) + 4\sqrt{3}(\epsilon e^{\frac{t}{2}}) e^{-2t}(\sigma_- \nu_- + \sigma_\times \nu_\times) + (\epsilon e^{\frac{t}{2}}) e^{-2t}(\nu_- \bar{\Sigma}_\times' + \nu_\times \bar{\Sigma}_-')]. \quad (22)$$

Clearly to second order we duplicate eqn. (21); the leading order correction to this eqn. comes from the term $\epsilon(\nu_- \bar{N}_\times + \nu_\times \bar{N}_-)$, which corresponds to eqn. (22) to next order. The remaining terms are of order $o(\epsilon e^{-2t})$ and $o(\epsilon^2)$. For early times $\partial_t \Omega_k > 0$, and so the magnitude of the spatial curvature grows. The sign of the next order terms is not necessarily positive.

2.2.5 Boundary conditions

We can consider PBC at $X = \pm L$. Any periodic initial data for any variable X on $[-L, L]$, for L sufficiently large, can be Fourier decomposed. Note that at $t = 0$ the average values are $\langle X \rangle = c_0$, which is usually taken to be zero, and $\langle X' \rangle = 0$. We are also interested in non periodic initial data, since in the formulation of G_2 models here PBC are not necessary

2.2.6 Numerical methods: Zooming

One numerical method for resolving small scale structure is adaptive mesh refinement (AMR). However, if we know beforehand the location of the structure, we need not use AMR. Because we wish to numerically study non-PBC, we shall consequently use zooming techniques, in which we use a coordinate system adapted to the structure that is under investigation. In particular, we can choose a coordinate system that shrinks exponentially with time, in which the new coordinates zoom in on the worldline, and where the constant rate of focus A is controlled ($A = 1$ is the natural choice, which ensures a good excision boundary throughout the simulation) [22]. The numerical grid ends at a fixed coordinate value $X = L$. Ordinarily, that would call for a boundary condition at L , but we can use the method of excision, which can be applied to any hyperbolic equations where the outer boundary is chosen so that all causal influences are outgoing. In that case the equations of motion are simply implemented at the outer boundary; no boundary condition is needed (or even allowed).

3 Results

In Figures 1–3 we present three numerical simulations for the G_2 dust evolution system in terms of the timelike area gauge and using β -normalized variables with the initial conditions $\{E_1^1 = 1, \Sigma_- = \tilde{\Sigma}_-, N_\times = 0, \Sigma_\times = 0, N_- = 0, \Omega = 1 - \tilde{\Sigma}_-^2, v = 0.1\}$ (which actually correspond to *diagonal* G_2 models, with $\Sigma_\times = N_- = 0$ at all times) and with (a) $\tilde{\Sigma}_- = 0.01 \sin \pi x$ (b) $\tilde{\Sigma}_- = 0.01 \sin \pi x + 0.01$ (c) $\tilde{\Sigma}_- = 0.01 \sin \pi x + 0.01x$ (each zooming in at $x_{\text{zoom}} = 0, 0.25, 0.5$, plotted in blue, green, red, respectively). The domain is $x - x_{\text{zoom}}$ in $[-10, 10]$ with zooming, with t running from $t = 0$ to $t = 3$. The initial conditions can be interpreted as a perturbed open FL model (small Σ_-) that is also close to a flat FL model (small v). The numerical results demonstrate that for all initial conditions v grows from 0.1 to 0.4, taking the solution further (drifting) away from flat FL (regarded as a *saddle point* in the dynamical state space), regardless of the periodicity or aperiodicity of the initial conditions.

From the final frame in the Figs. it is clearly demonstrated that Ω_k is suppressed in Fig. 1(a) with periodic initial conditions, and the growth of Ω_k is evident when periodicity is broken in Fig. 1(c), which can be attributed to the non-periodic term $0.01x$ in the initial conditions for Σ_- . Note that this non-periodic term has a very large wavelength. However, the simulations Fig. 1(b) show that the presence of a constant term 0.01 in Σ_- is found to have a negligible effect on the spatial curvature N_\times and Ω_k , since the large background homogeneous term in the shear in this model (i.e., $\Sigma_- = 0.01 \sin \pi x + 0.01$, which is still periodic) does not pass into N_\times . Additional simulations with various initial conditions were not found to change the qualitative behaviour of these results.

4 Discussion

We have shown that in this particular G_2 model periodic initial conditions do indeed suppress the spatial curvature, and hence we have verified that their use implies a small spatial curvature a priori. More comprehensive numerical analysis is possible but, as we noted above, this may not directly improve the qualitative conclusions regarding more general 3D simulations.

Indeed, in the G_2 FOSH formulation of the evolution eqns., the variables are not metric variables and consequently the initial conditions are not specified on the metric functions. Hence the meaning

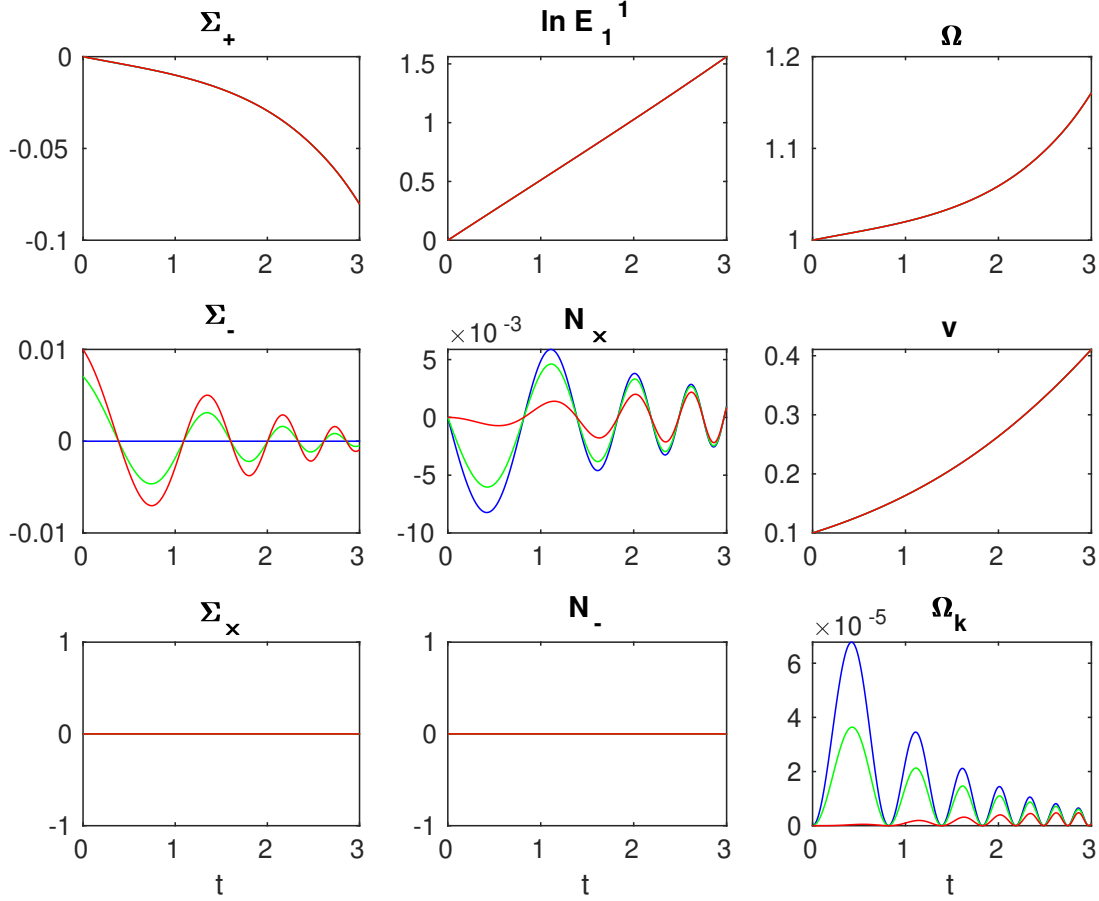


Figure 1: In Figure 1–3 we consider three numerical runs for the initial conditions (a) $\Sigma_- = 0.01 \sin \pi x$ (b) $\Sigma_- = 0.01 \sin \pi x + 0.01$ (c) $\Sigma_- = 0.01 \sin \pi x + 0.01x$ (each zooming in at $x_{\text{zoom}} = 0, 0.25, 0.5$, plotted in blue, green, red, respectively) in the diagonal G_2 models. The domain is $x - x_{\text{zoom}} \in [-10, 10]$, with t running from $t = 0$ to $t = 3$. The initial conditions can be interpreted as a perturbed open FL model (small Σ_-) that is also close to a flat FL model (small v). For all initial conditions v grows from 0.1 to 0.4, taking the solution further away from the flat FL model. The growth of the spatial curvature is displayed in the final frame in each figure for each initial condition.

of periodic initial data has a different meaning to that in the usual standard sense. Indeed, in this formulation once the initial conditions are fully specified the application of spatial boundary conditions are not even required. It is difficult to compare directly with the results obtained in the usual full 3D numerical simulations. Hence it is important to repeat this type of analysis in general cosmological simulations [12].

If the periodic initial conditions are maintained, the only arbitrarily large wavelength modes allowed are the background homogeneous terms, and they are only allowed in the shear components (which are time derivatives of the metric) but not in the spatial curvature components (which are spatial derivatives of the metric). That is, the spatially homogeneous growing mode is turned off, and long-wavelength modes which behave like Bianchi dynamics, leaving only short-wavelength modes which grow slower (if they grow at all). Periodicity generally disallows arbitrarily large wavelengths in the spatial curvature.

In the analysis there is a potential gauge issue which concerns the choice of the timelike area gauge (which affects the normalization of the independent variables such as Ω_k). (The usual gauge issues when using LPT are not relevant here in the numerical simulations). The emphasis in this short paper is to qualitatively illustrate the relative growth of Ω_k in the evolutions without PBC compared to those with PBC. Other numerical investigations were undertaken, but none challenge this conclusion and none, in our opinion, really led to any further insights. So although the gauge affects the actual quantitative results, it does not affect the qualitative results (at least according to our computations). In particular,

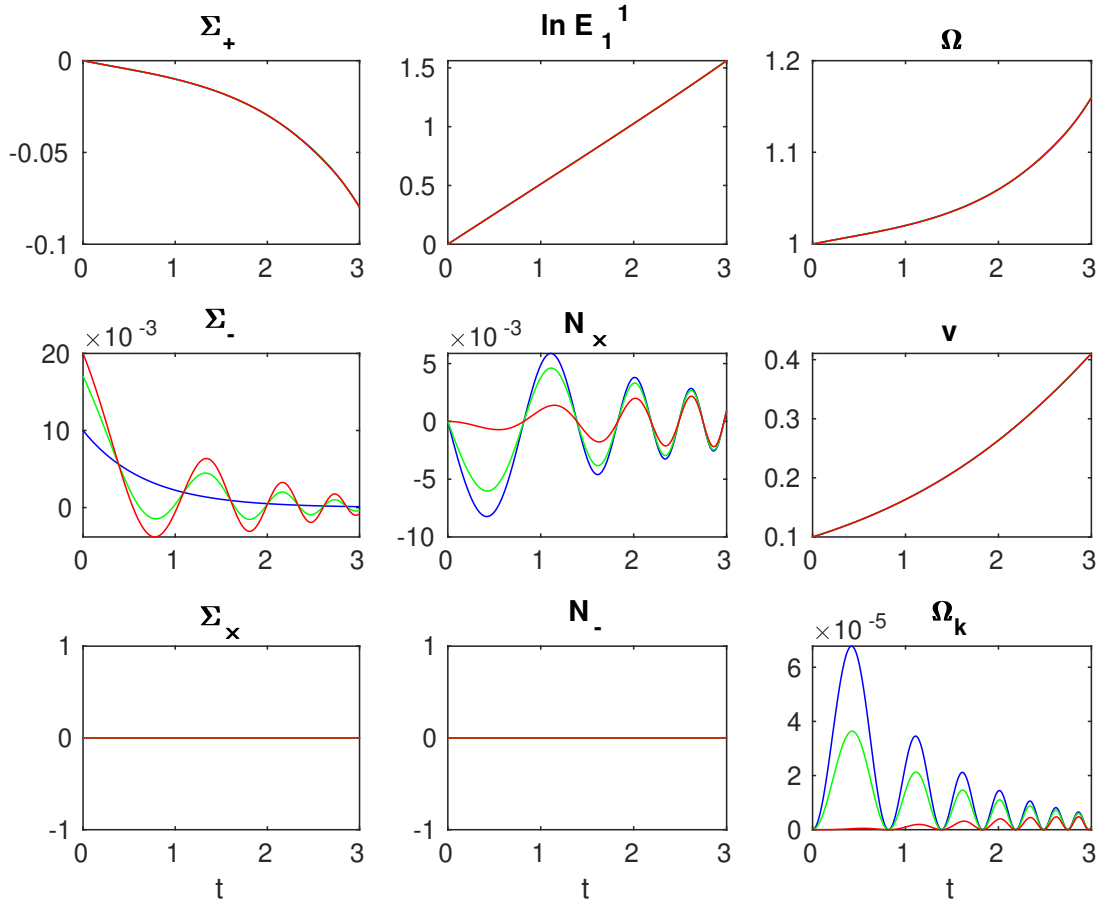


Figure 2: (See Figure 1 caption.)

the behaviour of the growth of Ω_k (in the figures) is typical as found across the region of simulation, and in other timelike area gauge numerical simulations, indicating that the relative average spatial curvature is increasing in the models without PBC. In addition, comparison of Ω and Ω_k in the figures (where the influence of the normalization factor is then minimised) illustrates that the qualitative growth of Ω_k in the evolutions without PBC compared to those with PBC does not depend on the choice of the timelike area gauge.

Data availability statement

The data that support the findings of this study are openly available at the following URL/DOI:

www.math.waikato.ac.nz/~wclim/pbcpaper2023_source_files/.

Acknowledgement

AAC would like to acknowledge NSERC for financial assistance. We would like to thank Pierre Mourier and Hayley Macpherson for helpful comments and private communications.

References

- [1] A. A. Coley and G. F. R. Ellis, *Class. Quant. Grav.* **37** 013001 (2020) [arXiv:1909.05346].
- [2] J. Martin [arXiv:1902.05286].

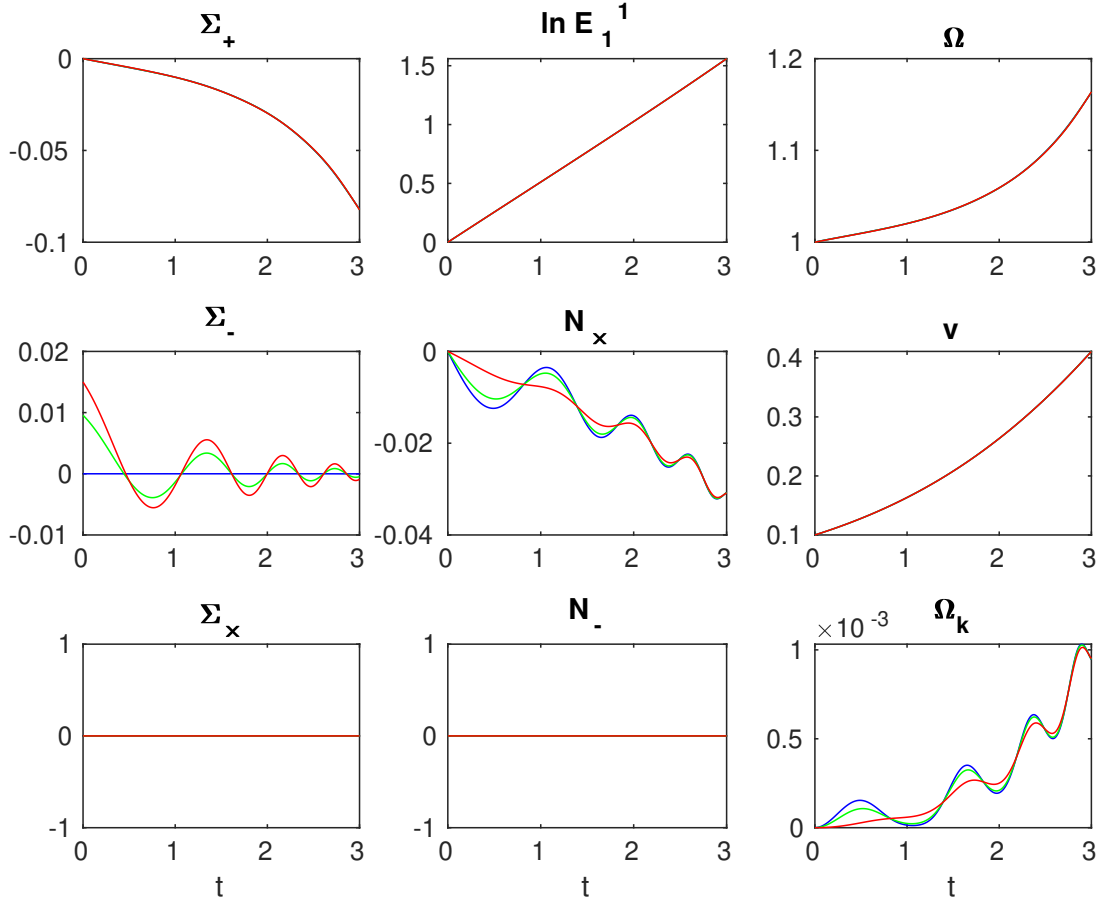


Figure 3: (See Figure 1 caption.)

- [3] Planck Collaboration: Planck 2018 results, *Astronomy & Astrophysics* **641** A6 & A7 (2020); Y. Akrami et al. [arXiv:1807.06205 & 06209 & 06211];
- [4] T. Buchert et al., *Int. J. Mod. Phys. D* **25** 1630007 (2016).
- [5] A. G. Riess et al., A Comprehensive Measurement of the Local Value of the Hubble Constant with 1 km/s/Mpc Uncertainty from the Hubble Space Telescope and the SH0ES Team [arXiv:2112.04510]; A. G. Riess et al., *Astrophys. J.* **861** 126 (2018) [arXiv:1804.10655].
- [6] E. Di Valentino et al., *Class. Quant. Grav.* **38** 153001 (2021); M. Asgari et al., *Astronomy & Astrophysics* **645** A104 (2021); T. M. Abbott et al., *Phys. Rev. D* **105** 023520 (2022).
- [7] A. Kashlinsky et al., *Astrophysical Journal Letters* **686** L49 (2008); C. Howlett et al., *Monthly Notices of the Royal Astronomical Society* **515** 953 (2022).
- [8] K. Bolejko, *Phys. Rev. D* **97** 103529 (2018); D. L. Wiltshire, *New J. Phys.* **9** 377 (2007) & *Class. Quant. Grav.* **28** 164006 (2011); T. Buchert et al., *Class. Quant. Grav.* **32** 215021 (2015); A. Coley, N. Pelavas and R. Zalaletdinov, *Phys. Rev Letts.* **95** 151102 (2005).
- [9] J. T. Giblin Jr, J. B. Mertens, G. D. Starkman and C. Tian, *Phys. Rev. D* **99** 023527 (2019) [arXiv:1810.05203 [astro-ph.CO]]; P. K. Aluri et al., Is the observable universe consistent with the cosmological principle? [arXiv:2207.05765].
- [10] H. Friedrich and A. Rendall. "The Cauchy problem for the Einstein equations." *Einstein's Field Equations and Their Physical Implications: Selected Essays in Honour of Jürgen Ehlers* (Springer, Berlin Heidelberg, pp 127-223, 2000).

- [11] H. Macpherson, J. Price and P. Lasky, *Phys. Rev. D* **99** 3522 (2019).
- [12] H. Macpherson and P. Mourier, in preparation.
- [13] J. Wainwright and G. F. R. Ellis (eds) *Dynamical Systems in Cosmology* (Cambridge Cambridge University Press, 1997).
- [14] H. van Elst, C. Uggla, and J. Wainwright, *Class. Quant. Grav.* **19** 51 (2002) [arXiv:gr/qc/0107041].
- [15] R. H. Gowdy, *Phys. Rev. Lett.* **27** 826 (1971) & *Ann. Phys. (N.Y.)* **83** 203 (1971).
- [16] M. Grasso, E. Villa, M. Korzyński and S. Matarrese, *Isolating non-linearities of light propagation in inhomogeneous cosmologies* [arxiv/2105.04552].
- [17] E. Villa, S. Matarrese, and D. Maino, *JCAP* **2011** 024 (2011).
- [18] J. Adamek, E. Di Dio, R. Durrer and M. Kunz, *Phys. Rev. D* **89** 063543 (2014).
- [19] V. A. Belinskii, I. M. Khalatnikov, and E. M. Lifshitz, *Adv. Phys.*, **12** 185 (1963) & **19** 525 (1970) & **31** 639 (1982).
- [20] B. K. Berger and V. Moncrief, *Phys. Rev. D* **48** 4676 (1993); B. K. Berger and D. Garfinkle, *Phys. Rev. D* **57** 4767 (1998); B. K. Berger, J. Isenberg and M. Weaver, *Phys. Rev. D* **64** 084006 (2001); D. Garfinkle, *Phys. Rev. Lett.* **93** 161101 (2004).
- [21] L. Andersson, H. van Elst, W. C. Lim and C. Uggla, *Phys. Rev. Lett.* **94** 051101 (2005).
- [22] W. C. Lim, L. Andersson, D. Garfinkle and F. Pretorius, *Phys. Rev. D* **79** 123526 (2009) [arXiv:0904.1546].
- [23] W. C. Lim, Ph.D. thesis, University of Waterloo 2004) [gr-qc/0410126].
- [24] H. van Elst and C. Uggla, *Class. Quant. Grav.* **14** 2673 (1997).